Applied Physics Letters ARTICLE scitation.org/journal/apl

Particularities of shocks generated by underwater electrical explosions of a single wire and wire arrays

Cite as: Appl. Phys. Lett. **115**, 074101 (2019); doi: 10.1063/1.5115134
Submitted: 14 June 2019 · Accepted: 16 July 2019 ·
Published Online: 12 August 2019

A. Rososhek,[a] S. Efimov, A. Virozub, D. Maler, and Ya. E. Krasik

AFFILIATIONS

Physics Department, Technion, Haifa 3200003, Israel

[a]sasharos@campus.technion.ac.il

ABSTRACT

The results of experimental and numerical research of shockwaves generated by the underwater electrical explosion of a single wire and a planar wire array are reported. Experiments were conducted using a microsecond time scale pulse power generator delivering a <210 kA current with a <1 μs rise time. Streak and fast framing cameras were used to study the time- and space-resolved evolution of the shocks. The results show that (a) an aperiodic discharge constitutes the most efficient method of generating a shockwave; (b) in the case of a planar wire array, an almost simultaneous explosion can be obtained when the individual wire diameter is <100 μm (current density $>2\times10^7$ A/cm^2); (c) the planar shock velocity can be accelerated using the combustion properties of the Al wires efficiently, and (d) the shock velocity can be enhanced using a metal reflector placed below the array.

Research on the underwater electrical explosion of single wires and wire arrays[1,2] showed that this approach can be used for studies[3–5] of warm dense matter and strong shockwaves (SSW), generated by these explosions. Indeed, recent studies[2] employing moderate pulse power generators with the stored energy of ≤6 kJ showed that the converging shock generated by an underwater electrical explosion of either quasi-spherical or cylindrical wire arrays results in an extreme state of water characterized by pressure $\geq10^{11}$ Pa, density ≥3 g/cm^3, and temperature ≥3 eV in the vicinity of the shock implosion. The measured energy deposition into the wire/array and the $\leq24\%$ efficiency of energy transfer into the water flow[2] are used as input parameters for one-dimensional[2] (1D) or two-dimensional[2] (2D) hydrodynamic (HD) simulations coupled with the equation of state (EOS) for the wire material and water.[6] The water parameters in the vicinity of the implosion are determined by fitting the simulated and experimental time-of-flight or the shock trajectory. In these studies, an almost critically damped discharge of the wire explosion was assumed to constitute the most efficient method for generating shockwaves. Also, it was assumed that the discharge current redistributes evenly between the wires in the array, leading to simultaneous wire explosions. However, neither of these assumptions was confirmed by the experimental data. Another important issue is related to the increase in water flow energy when combustion of Al wires is used, which was shown in a recent study.[7] However, straightforward experiments to show such a possibility were not conducted.

In this letter, we present the results of experimental studies of shocks generated by single wire and wire array microsecond-time scale underwater electrical explosions. The results of these experiments show that (a) a critically damped discharge indeed constitutes a more efficient method of generating shockwaves than an underdamped discharge; (b) in the case of a planar wire array, an almost simultaneous explosion can be obtained when the individual wire diameter is <100 μm (current density $>2\times10^7$ A/cm^2); (c) the combustion of Al wires in a planar array allows supplementary energy to be injected into the water flow, and (d) the shock velocity can be enhanced using a metal reflector placed below the array.

The experiments were conducted using a microsecond-time scale pulse generator[2] based on four low-inductance capacitors, connected in parallel with a total capacitance of ~10 μF. Each capacitor has its own multigap gas spark switch with capacitive coupling triggering. The generator stored energy was ~3.1 kJ at a charging voltage of 25 kV. When the inductance of the short-circuit load was 17 nH, the generator produced a current pulse of ~280 kA with a rise time of ~1.25 μs. In experiments with single wires, a 45 mm-long Al wire, of a diameter ranging from 100 μm to 800 μm, was placed coaxially inside a de-ionized water-filled chamber having ~4.5 cm diameter optical

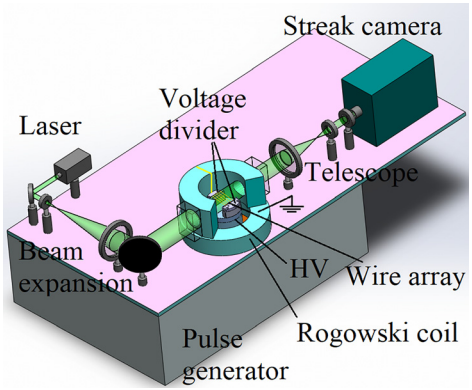

FIG. 1. Experimental setup.

windows. In the case of a 40 mm long planar array, the diameter of each Al or Cu wire was varied from 50 μm to 300 μm, and the number of wires in the array was varied from 4 to 50. A wire array was placed parallel to the high-voltage electrode and perpendicular to the laser beam.

The experimental setup is shown in Fig. 1. A diode-pumped 532 nm, 150 mW CW laser was used for backlighting the exploding wire and generated shock. The shadow images were obtained with a streak Optronis Optoscope SC-10 camera and a Stanford optics XXRapidFrame ICCD framing camera. The discharge current I and voltage drop φ across either a single wire or an array were measured with a Rogowski coil and a Tektronix voltage divider, respectively. At least two shots of the generator were captured for each experimental configuration ascertaining the reproducibility of the waveforms and the shadow images.

Waveforms of the discharge current and the calculated energy deposition for explosions of single Al wires having different diameters are shown in Fig. 2. The energy deposition into the wires was computed as $\epsilon(t) = \int_0^t I \times (\varphi - LdI/d\tau)d\tau$, where L is the load's inductance. Figure 2(a) suggests that an almost critically damped discharge is obtained only for the explosion of an 800 μm Al wire. This discharge is characterized by an ~1 μs long (at 10%–90% of maximal deposited energy) energy deposition into the wire and the formation of a low-ionized plasma channel with high resistivity. For 380 μm and 127 μm diameter Al wires, electrical explosions are delayed by $t < 0.7$ μs and $t < 0.15$ μs, respectively, relative to $t = 0$ of the discharge current.

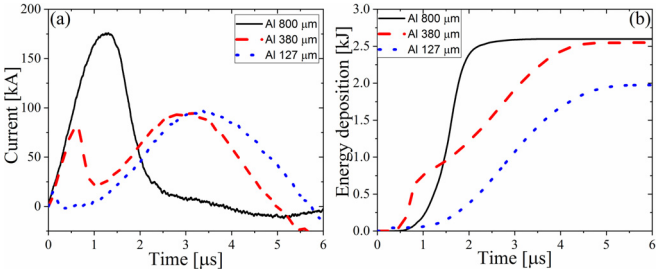

FIG. 2. Waveforms of the discharge current (a) and energy deposition (b) for the explosions of 800 μm, 380 μm, and 127 μm diameter Al wires.

These explosions are also followed by a decrease in the current because of the formation of a low-ionized high resistivity plasma. However, the significant part of the stored energy remained in the capacitors and the expansion of the plasma channel led to a current restrike. These explosions are characterized by a significantly longer ($\geq$3.1 μs) energy deposition into the discharge channel.

A typical shadow image of the diverging shock and a plasma channel obtained with an 800 μm Al wire explosion is shown in Fig. 3(a). Qualitatively similar shadow images were acquired in explosions of Al wires with other diameters. The algorithm used to obtain the time-dependent shockwave trajectory[8] consists of first marking the water–shockwave boundary, and then employing a MATLAB code; we scan this boundary at constant time steps. This results in a time-dependent shockwave trajectory. Differentiation of this trajectory results in the shockwave velocity. The fastest shock, i.e., $\sim 3 \times 10^5$ cm/s at $t \approx 2.3$ μs, as can be seen in Fig. 3(b), was observed in an Al 800 μm wire explosion, which is characterized by an almost critically damped discharge. In this case, a significant part (~1 kJ) of the stored energy was deposited into the wire during the vapor–low-ionized plasma phase transition. This phase transition occurs when $t \in (1.30, 1.65)$ μs, i.e., between the maxima of the discharge current and the resistive voltage when the channel's resistance reaches ~0.2 Ω. For a 380 μm diameter Al wire explosion, this time interval is ~140 ns and features only ~320 J deposited into the wire. Thus, one can state that the rapid deposition of a major part of the stored energy during the vapor–low-ionized plasma phase transition and, consequently the largest peak power deposited into the wire, is a key parameter for efficient shock generation, probably because the radial expansion of the exploding wire is the fastest.

Next, we describe the experimental results for the explosion of planar arrays, with various numbers of Cu wires of different diameters. These results allow us to measure the time delay in explosions of individual wires, δt, which can occur, for instance, when the current distribution among the wires is nonuniform. This is important to ensure that the shock resulting from the overlap of shocks generated by the individual wires explosions is uniform. In Fig. 4, we present the streak images of different planar array explosions, where the total mass of an array was kept constant, whereas the number of individual wires, N, and their diameter, d, were changed. In these experiments, the array configurations tested were $N \times d = 4 \times 300$ μm, 10×200 μm, and 14×130 μm Cu wires. To measure δt, we used the onset of weak shocks, generated when each wire undergoes a phase transition.[9] In

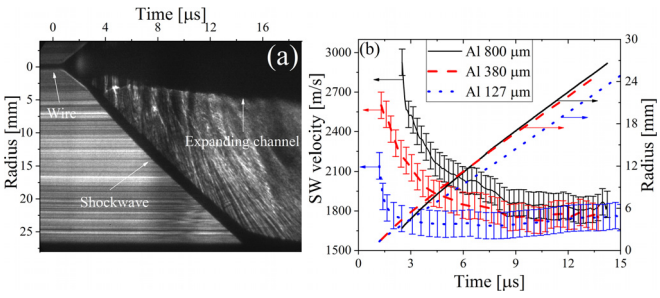

FIG. 3. Backlighted streak image of an exploding single Al wire of 800 μs diameter (a). The computed velocities (left axis) and the measured shock trajectories (right axis) generated by explosions of Al wires of different diameters (b).

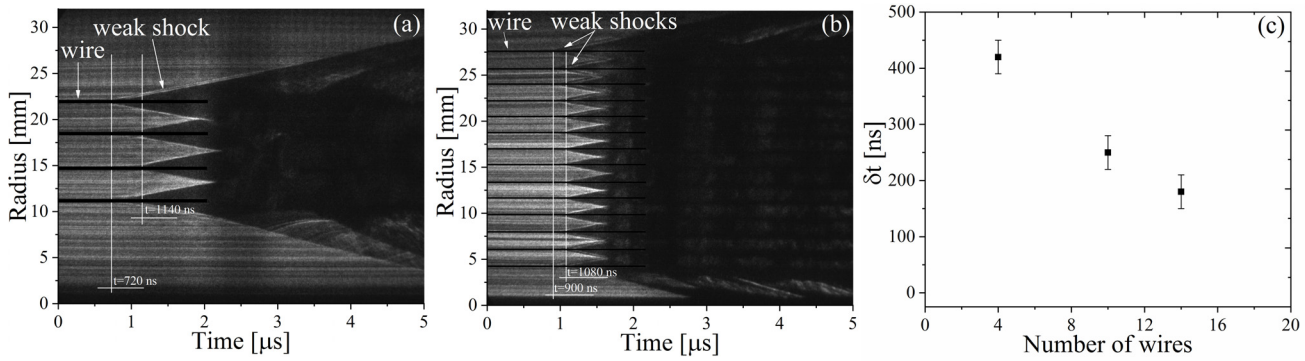

FIG. 4. Backlighted streak images of planar arrays with different numbers of wires and diameters of each wire [(a) and (b)]; time delay dependence on the number of wires in an array (c).

these experiments, the wire array was placed perpendicularly to the ground plate, such that the lowest wire (uppermost on the streak image in Fig. 4) was closest to the high-voltage electrode. One can see in Fig. 4 that the largest value, $\delta t \approx 420 \pm 30$ ns, is for the 4×300 μm array and the smallest, $\delta t \approx 190 \pm 30$ ns, for the 14×130 μm array explosions.

Several phenomena can be responsible for this dependence. (a) Because of the larger electric field at the transverse boundaries of the array, one can expect a larger current than through the wires located in the middle of the array. (b) The noncoaxial geometry of the array leads to different inductances of the discharge circuit for each wire, leading to the largest current in the wire having the smallest inductance [see the upper wire in Figs. 4(a) and 4(b)]. (c) An increase in d and a smaller N lead to a nonuniform current density radial distribution through the skin effect, leading to a slower increase in the resistance of an individual wire. This causes a delay in the current redistribution to the neighboring wires having a lower temperature and resistance. The dependence of the time delay on N in Fig. 4(c) suggests that, for wire arrays with $d < 100$ μm and $N > 20$, one can expect $\delta t < 100$ ns, which corresponds to the initial nonuniformity of the SSW front of only $\sim$200 μm for a typical shock velocity of 2×10^5 cm/s. Earlier research[10] showed that individual shocks generated by an explosion of a cylindrical 20×50 μm Cu wire array appeared almost simultaneously. Thus, when exploding the 50×50 μm Al planar wire array, one might expect a negligibly small δt between individual wire explosions.

In addition to the nonsymmetrical current distribution among the wires, one can argue that the planarity of the shock front is conserved only along small distances from the exploding array because of its finite width. This leads to a transformation of the planar shock to a quasisphere at some distance from the array. Using an XXRapidFrame camera to obtain the 90° rotated view of the shock and comparing this with a streak image, we confirmed the planarity of the shock front up to a distance of 2.5 cm from the 4 cm wide, 50×50 μm Cu wire array. A decrease in the 20×100 μm Cu wire array width to 2 cm showed that at a distance of 2.5 cm, the shock converts to a quasispherical shape.

Finally, we present the results showing that Al combustion can be used to increase the water flow energy generated by the explosion of an Al wire array. Recently, using time-resolved spectroscopy,[7] the ignition of Al shortened to $\sim$2 μs was demonstrated when an underdamped electrical discharge accompanied by a high-conductivity plasma formation was realized. This was explained qualitatively by the formation of the gas-plasma state, characterized by a temperature exceeding 10^3 K significantly and a relatively slow radial wire expansion. The latter allows Al gas-plasma to mix with water molecules, leading to a chemical combustion reaction, not only at the wire's surface but also in the bulk of the discharge channel. In the present experiments, the propagation of shocks generated by 40×127 μm and 50×50 μm Al wire arrays of 40 mm width was studied using streak shadow images. The explosion of a 40×127 μm array, where the cross-sectional area of all the wires is equal to one of the $\sim$800 μm Al wires, was almost critically damped in contrast to the 50×50 μm Al wire array explosion characterized by an underdamped discharge. In Fig. 5(a), one can see the trajectories/velocities of the shocks calculated from the streak images of Al array explosions. In the same figure, we present the results obtained by 2D hydrodynamic simulation for the explosion of a 16×90 μm Al wire array coupled with the SESAME EOS for water and the wire material. The total effective radius of this array is almost equal to that used in the experiment, i.e., $\sim$180 μm, and the energy density deposition is the same as for a 50×50 μm Al

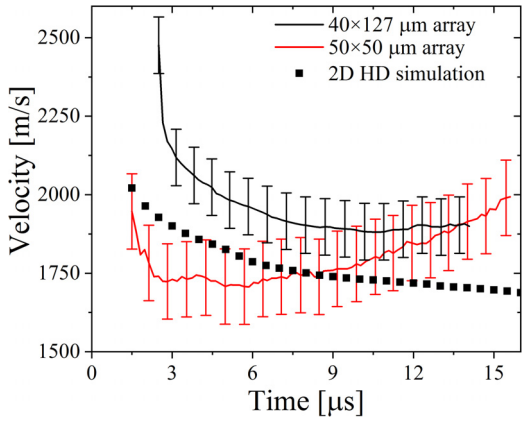

FIG. 5. The time-dependent velocity of the shocks generated by 40×127 and 50×50 μm Al wire array explosions, together with the simulated velocity (a).

wire array. Simulation of the experimental wire array with reasonable time and space resolution is too time consuming, and so a different array was used in the 2D HD simulations. Thus, the comparison of the simulated and experimental shock velocities is to be considered only qualitatively. The results of the experiments and simulations are shown in Fig. 5. One can see that in a $40 \times 127\,\mu$m Al wire array explosion, the shock velocity decreases quickly during the first $\sim 4\,\mu$s (up to a 0.730 ± 0.015 cm propagation distance). Then, this decrease becomes slower, and during 7–13 μs (up to 2.430 ± 0.015 cm), the shock velocity remains almost constant, in disagreement with the results of the study described in Ref. 8, where a slower shock decay was obtained and explained by continuing channel expansion. In the case of a $50 \times 50\,\mu$m Al wire array explosion, we have a pronounced contradiction with both the results of HD modeling that show a gradual decrease in the shock velocity and the previously published results.[8] Indeed, after the fast decrease in the shock velocity followed by a plateau during 3–6 μs, one obtains an increase in the velocity. The plateau in the shock velocity, and especially its further increase for $t > 6\,\mu$s (distance > 0.5 cm from the array), can be explained only by the supplementary energy source that delivers extra energy to the generated water flow. This added energy in our experiments can be due only to Al combustion, the ignition and efficiency of which are the largest for an underdamped discharge.[7] This also explains the reason for obtaining only a plateau in the velocity without a further velocity increase for a $40 \times 127\,\mu$m Al wire array explosion, when the Al combustion is delayed and less efficient, in contrast to a $50 \times 50\,\mu$m Al wire array explosion characterized by an underdamped discharge.

An additional increase in the shock velocity can be obtained placing a metal reflector below the array. The distance between the reflector and the array should be minimized to allow the reflected shock to contribute to the induced water flow, but this distance should be sufficiently large to prevent breakdown between the reflector and the wires. In our microsecond-time scale experiments with a 4 cm wide planar $36 \times 100\,\mu$m Cu wire array, the smallest distance was ~ 0.7 mm. Despite a breakdown around the resistive voltage maximum, the obtained shock velocity boost is about 5% or $\sim 8\%$ to the pressure behind the shock. Note that increasing the gap to ~ 1 mm and obtaining $\sim 30\%$ larger energy deposition without a breakdown do not lead to further velocity increase, i.e., the increment is again 5%.

To summarize, we conducted experiments on underwater electrical explosions of single wires and planar Al wire arrays using a microsecond-time scale generator and showed that (a) the highest shock velocity is achieved when the generator's discharge is almost critically damped, (b) to achieve an almost simultaneous wire array explosion, the wires' diameter should be $<100\,\mu$s (current density $>2 \times 10^7$ A/cm^2), (c) one can accelerate the planar shock velocity by using efficient combustion of Al wires, and (d) the shock velocity can be enhanced using a metal reflector placed below the array.

We thank Dr. V. Gurovich and Dr. J. Leopold for fruitful discussions and S. Gleizer for her generous technical assistance. This research was supported by the Israeli Science Foundation Grant No. 492/18 and in part by the Center for Absorption in Science, Ministry of Immigrant Absorption, the State of Israel.

REFERENCES

[1]A. W. DeSilva and J. D. Katsouros, Phys. Rev. E **59**, 3774 (1999).
[2]Ya. E. Krasik, S. Efimov, D. Sheftman, A. Fedotov-Gefen, O. Antonov, D. Shafer, D. Yanuka, M. Nitishinskiy, M. Kozlov, L. Gilburd, G. Toker, S. Gleizer, E. Zvulun, V. Tz. Gurovich, D. Varentsov, and M. Rodionova, IEEE Trans. Plasma Sci. **44**, 412 (2016) and references therein.
[3]V. E. Fortov and I. T. Iakubov, *The Physics of Non-Ideal Plasma* (World Scientific, Singapore, 2000).
[4]A. W. DeSilva and H.-J. Kunz, Phys. Rev. E **49**, 4448 (1994).
[5]J. Stephens, J. Dickens, and A. Neuber, Phys. Rev. E **89**, 053102 (2014).
[6]S. P. Lyon and J. D. Johnson, "SESAME: The Los Alamos National Laboratory equation-of-state database," Report No. LA-UR-92–3407 (Los Alamos National Laboratory, 1992).
[7]A. Rososhek, S. Efimov, A. Goldman, S. V. Tewari, and Ya. E. Krasik, Phys. Plasmas **26**, 053510 (2019).
[8]A. Rososhek, S. Efimov, V. Gurovich, A. Virozub, S. V. Tewari, and Ya. E. Krasik, Phys. Plasmas **26**, 042302 (2019).
[9]A. Rososhek, S. Efimov, S. V. Tewari, D. Yanuka, and Ya. E. Krasik, Phys. Plasmas **25**, 102709 (2018).
[10]D. Yanuka, A. Rososhek, S. N. Bland, and Ya. E. Krasik, Appl. Phys. Lett. **111**, 214103 (2017).